Study of Spray-Cooling Control to Maintain Metallurgical Length During Speed Drop in Steel Continuous Casting

Zhelin Chen[1], Joseph Bentsman[1], Brian G. Thomas[2], Akitoshi Matsui[3]

[1]University of Illinois at Urbana-Champaign
1206 W Green St, Urbana, IL, USA, 61801
Phone: 217-418-4714
Email: zchen61@illinois.edu

[2]Colorado School of Mines
1610 Illinois St, Golden, CO, USA, 80401

[3]JFE Steel Corporation
Steel Research Lab, 1 Kokan - cho, Fukuyama, Hiroshima, 721-8510, Japan

Keywords: continuous casting, solidification, spray-cooling control, metallurgical length, segregation

ABSTRACT

For operations limited by the casting speed, or for steel grades more sensitive to centerline rather than surface defects, the control of metallurgical length is very important. Operations designed to reduce centerline defects, such as soft reduction, are affected greatly by transient changes in the metallurgical length. This work explores the potential of using open-loop spray-cooling control methods to minimize deviations in the metallurgical length from its desired location, during casting speed changes under temperature setpoint constraints. This objective essentially reduces to motion planning, i.e. apriori generation of spray flow rate commands that when applied to the process make the latter execute the motion that carries out the above task in the shortest time possible. The results show that there is only a small potential to maintain metallurgical length during speed changes in a 221mm thick slab caster. By changing spray water flow rates between their greatest and smallest conditions, it is possible to accommodate casting speed variations from 1.7 to 1.5 m/min, while maintaining a constant metallurgical length of 22.29 m during steady casting. For a sudden speed drop, however, a dip in metallurgical length is unavoidable. Bang-bang control was the best method investigated to manage water sprays during the transition. This control method can lessen the dip JFEin metallurgical length from over 2m (with no control), to less than 1m.

INTRODUCTION

In continuous casting of steel, strand surface temperature profile and metallurgical length are two key processing variables that require real-time control to meet product quality and operational safety demands. The main focus of the control methods currently used in the steel industry is to maintain steel surface temperature in each spray zone down the caster. One of the most common control methods for secondary cooling is “spray table” control, which is also called “speed-based” control. In this method, the spray flow rates are interpolated from a look-up table, according to the current casting speed and the given spray pattern. The spray pattern defines the flow rates in each spray zone for each casting speed in the table, and depends on the steel grade, product dimensions, and machine design.

Another widely-used general class of control methods, is called “dynamic-spray” control. These control methods include the concept of cooling time [1] [1], and are actually improved versions of spray-table control. The original method has been called the residence time method, element lifetime method, or effective lifetime method [1] [1], and is referred to as “time-constant” control in this paper. A more general dynamic spray cooling method, which combines together the concepts of the spray table and cooling with time, is based on an empirical mixture constant, and is called the “effective speed” control method [2, 3] [2, 3]. Effective speed control finds an effective casting speed (weighted speed of the average casting speed and the current casting speed) and uses it to calculate the spray flow rates from a given spray pattern. The concept is to deliver the

same amount of water to each cross-section through the steel strand, according to the time that slice has spent in the caster. Thus, these control methods

smooth out the transient surface temperature fluctuations during sudden speed changes, relative to the sudden, detrimental temperature changes that occur with simple spray-table control [2] [2].

However, for operations limited by the casting speed, or for steel grades that are more sensitive to centerline defects than to surface defects, the control of metallurgical length may be more important. Centerline segregation is a type of macro-segregation that appears as a line of impurities, and is accompanied by porosity, inclusions, alloy-rich regions, and even cracks, distributed near the centerline along the slab length. These centerline defects are often very harmful, especially in highly-alloyed steels, or when the slab is rolled into thin plates [4] [4].

Soft reduction technology has been developed to reduce centerline segregation. As shown in Figure 1, during the solidification process, the steel shrinks the most while transitioning from liquid phase to solid phase. Therefore, the centerline is susceptible to segregation and other defects if the roll gap profile, which defines the taper of the entire casting machine, does not match the steel shrinkage. The choice of location of the soft reduction region depends on the shell thickness profile and the metallurgical length. If the steel is completely solid when the slab enters the soft reduction region, then the rolls experience large forces from the solid steel which could damage both the slab and the rolls. If the steel is insufficiently solid upon entering the region, then soft reduction is insufficient where it is needed and centerline defects will arise. The soft reduction operation performs best when the shell thickness profile and metallurgical length stay constant with time.

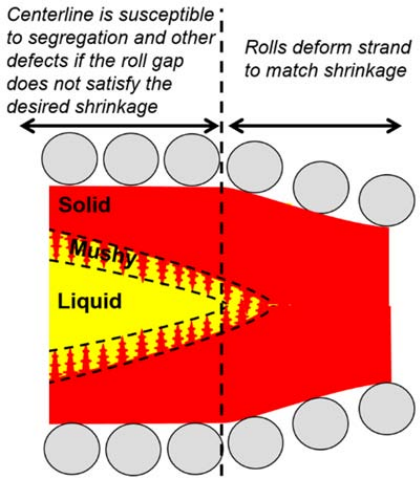

Figure 1. Soft reduction operation to reduce centerline segregation.

This paper explores the potential of using open-loop control methods for the task of maintaining the metallurgical length during casting speed changes, under temperature constraints using four different control methods for the secondary cooling. First, a brief survey of the control methods is given. A particular dynamic model, CONOFFLINE (off-line version of CONONLINE model [5][5]), has been calibrated with plant measurements and used to investigate the dynamic thermal behavior of a particular continuous steel slab caster during speed drops, under different secondary cooling control methods. The metallurgical length variations are compared for the different control methods.

CONTROL METHODS OVERVIEW

For secondary cooling, the performance of the following different control methods on controlling the metallurgical length during speed drops are explored: (1) constant spray cooling (no control); (2) spray-table control; (3) time-constant control; (4) bang-bang control.

Constant spray cooling

The spray flow rates in the secondary cooling region are kept constant during speed changes. This lack of any control is used as a reference to compare the performance of other control methods.

Spray table control

For spray table control, the spray-water flow rates in the different spray zones, or spray patterns, that produce good quality steel are determined by experience, plant trial and error, and steady state modeling. Higher casting speed requires higher

water flow rates to maintain same cooling conditions. These spray patterns depend on steel grade, production dimension, and machine design, and are tabulated as a function of casting speed. During the continuous casting process, if the casting speed changes, plant operators or an automatic level 2 control system will instantly change spray water flow rates by interpolating between the flow rates defined by the spray pattern for the casting speeds in the table above and below the actual casting speed.

Time-constant control

Under conditions of constant casting speed, the strand surface temperature at a given location z along the caster is constant and depends on the time it takes for the slice to reach that point from the meniscus, i.e. the "dwell time" of a slice, and the cooling conditions encountered. An increase in the casting speed will cause the dwell time to decrease, while the opposite will occur with a decrease in speed. The idea of time-constant control method is to change the flow rates according to the dwell time.

Consider the following general case: at wall-clock time t = 0, the caster starts casting and the steel is casting at time-varying casting speed $v_c(t)$, where z is an arbitrary location along the caster. The dwell time $\tau(z)$ is defined as the time taken for the steel to travel from the meniscus to location z at time t, and it can be found by solving the inverse of the following equation:

$$z = \int_{t-\tau(z,t)}^{t} v_c(s)ds \tag{1}$$

After calculating the dwell time, the average casting speed $\overline{v_c}$ for a slice to reach location z from the meniscus can be calculated from the following equation:

$$\overline{v}_c(z,t) = \frac{z}{\tau(z,t)} \tag{2}$$

In the continuous casting process, a spray zone typically can only have just one spray flow rate over the entire zone, so instead of average casting speed for location z, $\overline{v}_c(z,t)$, the average casting speed is calculated for spray zone i at time t, $\overline{v}_i(t)$:

$$\overline{v}_i(t) = \frac{z_{mid}(i)}{\tau(z_{end}(i),t)} \tag{3}$$

where $z_{mid}(i)$ and $z_{end}(i)$ are the distance from the meniscus to the middle and end of spray zone i,, and $\tau(z_{end}(i),t)$ is the dwell time for the steel to travel from the meniscus to the end of spray zone i. Then $\overline{v}_i(t)$ is used to lookup the spray flow rate for spray zone i from the spray table.

Bang-bang control

In control theory, the bang-bang optimal controller, also known as the hysteresis controller, is a controller that switches abruptly between two or more states [6] [6]. Consider a simple model of a car moving on a horizontal line. The driver wants to spend minimum time to move to a destination. The best solution is to apply maximum acceleration until a unique switching point and then apply maximum deceleration, which makes the car stop exactly at the destination. This is a simple example that needs a two-step bang-bang controller that switches abruptly between two states: maximum acceleration and maximum deceleration.

In this paper, bang-bang control was applied to the following optimization problem: control secondary spray cooling water to minimize the metallurgical length fluctuation during casting speed change within the spray flow rate constraints of each spray zone. Three different particular types of bang-bang control were investigated here: single-step bang-bang, two-step bang-bang, and three-step bang-bang control sequences. For single-step bang-bang control, the flow rates only switch once after the speed drop. At the optimal chosen time, t_{1b}^{i}, the flow rate at each spray zone switches from $Q_{sw}^{i}(orig)$ (the spray pattern before speed change) to $Q_{sw}^{i}(final)$ (the final spray pattern). Under single-step bang-bang control, the flow rate of spray zone i is calculated as follows:

$$Q_{sw}^{i} = \begin{cases} Q_{sw}^{i}(orig)\ if\ t < t_{1b}^{i} \\ Q_{sw}^{i}(final)\ if\ t \geq t_{1b}^{i} \end{cases} \quad (4)$$

where Q_{sw}^{i} is the spray cooling water flow rate in spray zone *i*, and t_{1b}^{i} is the switching time.

For two-step bang-bang control, the spray flow rate for each spray zone switches twice: after the speed drop, the flow rate first immediately switches to the minimum flow rate allowed, and then at a predetermined switching time, the flow rate switches to the value from the calibrated spray pattern for the final casting speed, denoted as $Q_{sw}^{i}(final)$. Under two-step bang-bang control, the flow rate of the spray zone *i* is found from:

$$Q_{sw}^{i} = \begin{cases} Q_{sw}^{i}(orig)\ if\ t < t_{2b1}^{i} \\ Q_{sw}^{i}(min)\ if\ t_{2b1}^{i} < t < t_{2b2}^{i} \\ Q_{sw}^{i}(final)\ if\ t \geq t_{2b2}^{i} \end{cases} \quad (5)$$

where t_{2b}^{i} are the two switching times and $Q_{sw}^{i}(final)$ is the final flow rate for spray zone *i*.

For three-step bang-bang control, the flow rate is found from:

$$Q_{sw}^{i} = \begin{cases} Q_{sw}^{i}(orig)\ if\ t < t_{3b1}^{i} \\ Q_{sw}^{i}(min)\ if\ t_{3b1}^{i} < t < t_{3b2}^{i} \\ Q_{sw}^{i}(3b)\ if\ t_{3b2}^{i} < t < t_{3b3}^{i} \\ Q_{sw}^{i}(final)\ if\ t \geq t_{3b3}^{i} \end{cases} \quad (6)$$

where t_{3b}^{i} are the three switching times, $Q_{sw}^{i}(3b)$ and $Q_{sw}^{i}(final)$ are the switching water flow rate and final flow rate for spray zone *i*. t_{3b}^{i} and $Q_{sw}^{i}(3b)$ can be controlled and need to be determined in advance. Under three-step bang-bang control, after the speed drop, the spray flow rate at spray zone *i* first drops to the minimum flow rate allowed $Q_{sw}^{i}(min)$, then at time t_{3b2}^{i}, the flow rate switches to $Q_{sw}^{i}(3b)$, and at time t_{3b3}^{i}, the flow rate switches to the final value $Q_{sw}^{i}(final)$.

In this work, the parameters $t_{b}^{i}, t_{2b}^{i}, t_{3b}^{i}, Q_{sw}^{i}(3b)$ for the above bang-bang control sequences were tuned based on the CONONLINE model prediction of the metallurgical length under corresponding bang-bang control sequences.

MODEL DESCRIPTION

A brief overview of the CONOFFLINE model, off-line version of the CONONLINE model that was described in [5][5], will be given in this section. The control diagram in Figure 2 is realized in CONOFFLINE. CONOFFLINE uses recorded or specific casting conditions as inputs for the software sensor (Consensor); and different control methods are applied to this model. CONOFFLINE can be used to investigate the behavior of casters, especially phenomena such as transient evolution of the shell thickness profile, which cannot be easily measured.

Software sensor

For a solidifying domain with heat transferred by internal conduction and advection, conservation of energy satisfies the following partial differential equation (PDE):

$$\rho c_{p}^{*}\left(\frac{\partial T}{\partial t} + \vec{v} \bullet \nabla T\right) = \nabla \bullet (k \nabla T) \quad (7)$$

where $T(x, y, z, t)$ is the temperature at a given point (*x*,*y*,*z*) in the cast strand and $\vec{v} = (v_x, v_y, v_z)$ is the velocity of the material at that point. For this work, *z* denotes the casting direction, *x* denotes the thickness direction (narrow face cross-sectional dimension) and *y* denotes the width direction (wide face cross-sectional dimension). The origin of the *x*- and *y*-axes

are at the center of the strand and the origin of *z*-axis is at the meniscus. The density ρ, the thermal conductivity *k*, and the effective specific heat c_p^* are the properties of the cast material. The effective specific heat includes the latent heat:

$$c_p^* = c_p + L_f \frac{df_s}{dT} \tag{8}$$

where c_p is the usual specific heat, L_f is the latent heat, and f_s is the solid fraction of the steel.

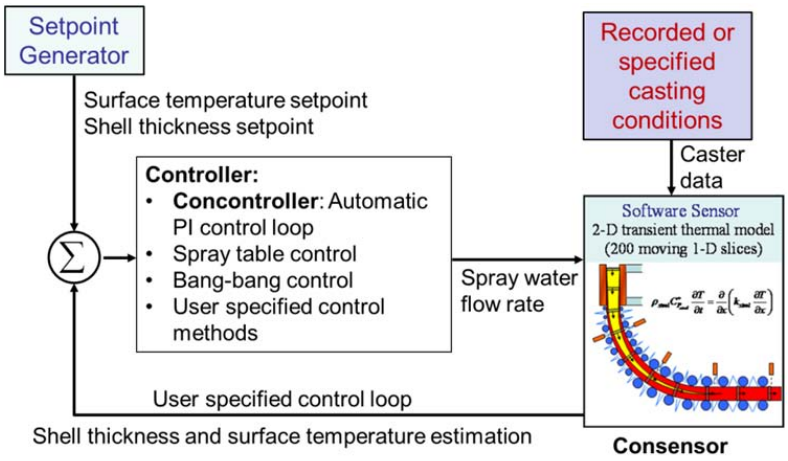

Figure 2. Control diagram of CONOFFLINE.

The material in the steel strand moves in the *z*-direction at casting speed v_c, and conduction in the *y*- direction only matters near the corners of the slab. With these simplifications, equation (7) simplifies to the following:

$$\rho c_p^* \left(\frac{\partial T}{\partial t} + v_z \frac{\partial T}{\partial z}\right) = \frac{\partial}{\partial x}\left(k \frac{\partial T}{\partial x}\right) + \frac{\partial}{\partial z}\left(k \frac{\partial T}{\partial z}\right) \tag{9}$$

The relative size of the remaining terms are compared through scaling analysis. The Peclet number,

$$Pe = \frac{v_c L_z \rho c_p}{k} \tag{10}$$

is the ratio of advection to conduction heat transfer rate in the *z*-direction, where L_z is the characteristic length in the casting direction. If L_z is taken to be the length of the whole caster, then take advantage of the large Peclet number, the conduction in the *z*-direction is negligibly small compared to the advection in the *z*-direction. Therefore, the conduction in the *z*-direction is safe to neglect, so the remaining terms in the equation (9) are:

$$\rho c_p^* \left(\frac{\partial T}{\partial t} + v_z \frac{\partial T}{\partial z}\right) = \frac{\partial}{\partial x}\left(k \frac{\partial T}{\partial x}\right) \tag{11}$$

Furthermore, the model takes the Lagrangian reference frame for its simulation domain: a slice through the slab thickness, which moves with the steel in the *z*-direction at the casting speed. Mathematically, instead of calculating $T(x,z,t)$, the model calculates $T(x,v_c t,t)$. Then, equation (11) becomes:

$$\rho c_p^* \frac{\partial T}{\partial t} = \frac{\partial}{\partial x}(k \frac{\partial T}{\partial x}) \tag{12}$$

Equation (12) could be solved faster than real time, but it only gives the temperature estimation at the locations of the moving reference frame, which in return depends on the casting speed history. By repeating the calculation for multiple slices simultaneously, CONSENSOR can produce the temperature profile along the entire caster (z) and through its thickness (x) in real time. It does this by managing the simulation of N different slices, each starting at the meniscus at different time to achieve a fixed z-direction spacing between the slices.

Currently, CONSENSOR manages exactly 200 slices, which corresponds to a uniform spatial interval of 0.255 m along the entire simulation domain for the illustrative example case based on the JFE thick-slab caster, z_{total}=51 m. After the first slice is created at the meniscus, whenever the most recent slice moves downward 0.255 m, a new slice is generated at the meniscus and starts moving downward. If an old slice moves out of the containment, a new slice starts from the meniscus. By using this method, there are always 200 slices in the whole caster after start up.

Model validation

The CONONLINE model was recently validated by Petrus [7] [7] for transient conditions. Specifically, the validation was done by comparing the simulation results of transient changes in the metallurgical length during casting speed changes with the plant measurements conducted on a 260 mm thick-slab caster at Burns Harbor during transient conditions [8] [8]. During the trial, strain gauges were installed on some of the support rolls to measure the changing forces exerted on those rolls by the strand.

Figure 9 in [7][7] compares the prediction results from CONSENSOR and the measurements, showing good qualitative matches between the measured roll forces and the predicted TLE (Thermal linear expansion) at the rolls. Especially, the figure shows quantitative match between the timing of changes in roll force and the timing of changes in the thermal linear expansion predicted by CONSENSOR. Readers may refer to [7][7] for more detailed information on validation of this model.

DYNAMIC SIMULATION

Casting conditions

The caster and casting conditions simulated in this work were based on the thick-slab (221 mm) caster at JFE Steel, Japan. The typical low-carbon steel grade studied in this work has the properties given in Table 1.

Table 1. Steel properties in simulation

Liquidus temperature	1516.10 $°C$
Solidus temperature	1468.40 $°C$
Peritectic temperature	1486.50 $°C$
Latent heat of solidification	271 kJ/kg

Based on an empirical correlation proposed by Duvvuri [9][9], the average heat flux in the mold was set to:

$$Q_m \left[MW / m^2 \right] = 1.2154 \left(v_c \right)^{0.47} \tag{13}$$

The coefficient and exponent were adjusted to match data from JEF Steel. More casting conditions are listed in Table 2. For the heat flux of the spray cooling water in the secondary cooling region, Nozaki's empirical correlation [10][10] was used:

$$h_{spray} = 0.3925 \times Q_{water}^{0.55} \times \left(1 - 0.0075 \times T_{spray} \right) \tag{14}$$

where Q_{water} (L/m^2) is water flux in the spray zones, T_{spray} is the temperature of the cooling water spray. The heat transfer in the secondary cooling region is a subject of ongoing research, and other relations are available and used at different casters (including JFE).

The speed change scenario simulated in this work is a sudden speed drop from 1.7 *m/min* to 1.5 *m/min*. However, in the real caster, there are limits of sudden speed drops that can be applied during the continuous casting process. If a sudden speed drop is too large, the flow-control system may be unable to maintain constant steel flow into the caster and cause problems such as severe level fluctuations and breakouts, especially for thick-slab casters. Therefore, when a large speed drop is needed during operation, the speed drop is made in several steps, or made gradually over a time interval (usually several seconds).

Table 2. Casting conditions of the JFE caster simuations

Property	**Value**	**Unit**
Density of solid steel, ρ	7400	kg/m^3
Steel emissivity, ε_{steel}	0.8	/
Solid fraction for shell thickness location, f_s	0.3	/
Specific heat of solid steel, c_p	670	$J/kg\bullet K$
Thermal conductivity of solid steel, k	30	W/mK
Thermal diffusivity of solid steel, α	6.0508×10^{-6}	/
Initial cooling water temperature, T_{water}	29.67	$°C$
Slab thickness, L_x	221	mm
Slab width, L_y	2095	Mm
Ambient temperature, T_∞	35	$°C$
Pouring temperature, T_{pour}	1545	$°C$
Time step	0.01	s
Mesh size	0.55	mm

The speed drop of 0.2 *m/min* studied in this work is small. The results of steady state simulation show that under this small speed drop, the same metallurgical length is achievable at these two casting speeds by applying feasible water flow rates. The limitations of spray flow rates for each spray zone, i.e. the maximum and minimum flow rates allowed, are listed in Table 3. At each spray zone, there are a series of rows of spray nozzles; the spray flow rates of spray zone *i*, denoted as Q_{sw}^i throughout this work, can be calculated by:

$$Q_{sw}^i = q_{sw}^i / m_r \tag{15}$$

where q_{sw}^i (*L/min*) is the total amount of water applied to spray zone *i*, m_r is the number of rows of spray nozzles in zone *i*, and Q_{sw}^i (*L/min/row*) is the water flow rate for each row of spray nozzles in spray zone *i*.

Table 3. Spray flow rates limitation of each spray zone

Zone	$Q_{sw}^i(max)$ (L/min/row)	$Q_{sw}^i(min)$ (L/min/row)
1	250.0	75.0
2	286.7	28.7
3	360.0	36.0
4	200.0	10.0
5	200.0	10.0
6	90.0	4.5
7	90.0	4.5
8	60.0	3.0
9	30.6	1.53
10	15.0	1.0
11	15.0	1.0
12	15.0	1.0

Table 4. Spray patterns that gives same metallurgical length

Zone	**1.7_*orig*** (L/min/row)	**1.5_*sameML*** (L/min/row)
1	90.2	75.0
2	61.9	55.0
3	98.2	56.6
4	127.9	40.0
5	111	30.0
6	70.9	20.0
7	51.0	14.4
8	19.1	5.0
9	6.0	3.9
10	4.1	3.4
11	3.6	2.8
12	6.5	5.6

In order to investigate the dynamic thermal behavior of the steel strand during changes between two specific speeds (1.5 *m/min* and 1.7 *m/min*), the original spray table was modified to make a hypothetical, but still realistic, example of a part of a spray table. Specifically, the water flow rates used in the plant at a casting speed of 1.5 *m/min* were changed to match the metallurgical length of 1.7 *m/min*, using the mold heat-flux equation (13), and Nozaki heat flux / water flow rate relation given earlier in equation (14).

For the secondary cooling region, three different control methods were applied to explore their performance on maintaining the surface temperature: constant spray cooling, spray table control, and bang-bang control. Before running simulations of different control methods, CONOFFLINE model was first calibrated according to provided casting conditions. Figure 3 shows the shell thickness profile under steady state for two casting speeds. The predicted metallurgical lengths of both speeds match the measured data. Figures 4 shows that the predicted surface temperatures agree with the measurements at steady state at these two casting speeds. After calibration, the CONONLINE model was ready to be used for further simulations.

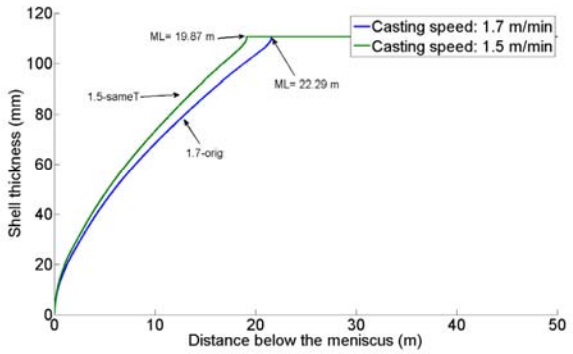

Figure 3. Shell thickness at steady state

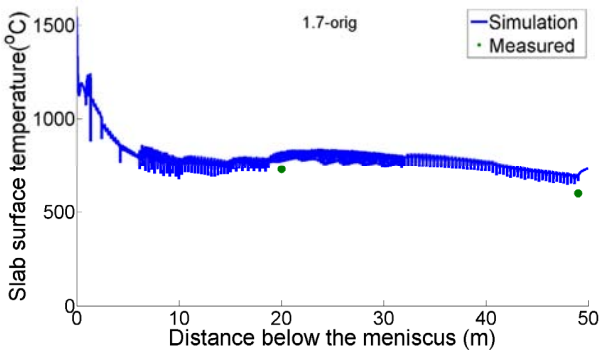

Figure 4. Surface temperature at steady state of 1.7 *m/min*

The hypothetical spray patterns given in Table 4 achieve the same metallurgical length under steady state conditions at two different casting speeds. The spray pattern '1.5_*sameML*' was determined by steady state simulations; the flow rates were chosen to match the metallurgical length under the spray pattern of '1.7_*orig*' at each casting speed.

Figures 5 shows the model predictions of the surface temperature histories and the shell thickness profiles under two different spray patterns: '1.7_*orig*', and '1.5_*sameML*'. Figure 5 shows that the shell thickness profile under the spray pattern of '1.5_*sameML*' is almost identical to the shell thickness profile under the spray pattern of '1.7_*orig*'. Therefore, the metallurgical lengths are the same with these two spray patterns at these two different casting speeds. The figure also indicates a large temperature difference between two steady-state temperature profiles with these two spray patterns, which is expected. Because it is not possible to maintain both surface temperature and metallurgical length to be constant during a speed change, severe changes of the surface temperature during the speed changes are not the main concern in this study.

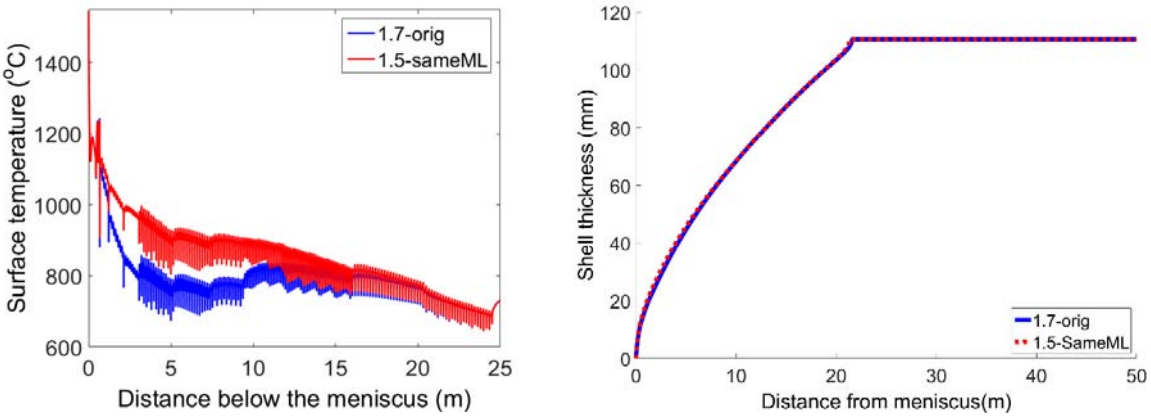

Figure 5. CON1D model prediction of surface temperature and shell thickness profile under different spray patterns.

The results in Figure 5 show that under the small speed drop of 0.2 *m/min* studied here, constant metallurgical lengths at both casting speeds are achievable by applying the largest feasible water flow rates possible under steady state conditions for this

caster. The metallurgical length deviation, defined as the difference (undershoot and / or overshoot) between the metallurgical length at 1.7 *m/min* and the final metallurgical length after the speed drop, is used to compare their performance. For all the simulations below, the speed change is assumed to happen at t=0.

Constant spray cooling (No spray control)

In order to compare the performance of different control methods, the 'no control' case was simulated first, keeping the spray flow rates everywhere in the secondary cooling region constant throughout the speed drop. The specific spray flow rates used are the values from the spray pattern of '1.7_*orig*'.

The model prediction of the metallurgical length after the speed drop is shown in Figure 6. After the speed drop, the metallurgical length decreases linearly. By 776 seconds after the speed drop, the steel is fully solid around 19.57 *m* and the maximum metallurgical length deviation is a decrease of 2.72 *m*.

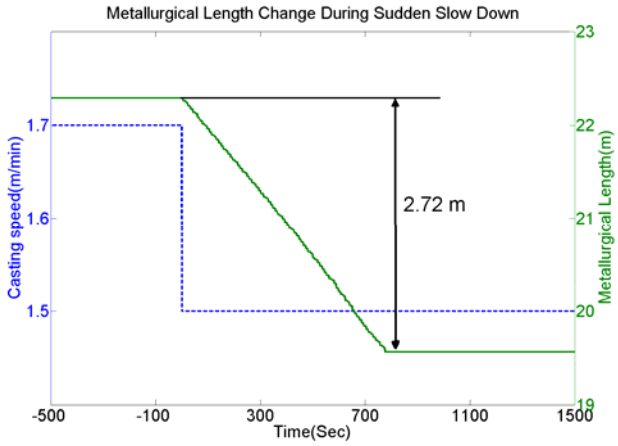

Figure 6. Model prediction of metallurgical length during the speed drop under constant spray cooling.

Spray table control

Applying spray table control to the secondary cooling region using the spray patterns given in Table 4 gives the following water flow rates equation:

$$Q_{sw}^{i}(t) = Q_{sw}^{i}(v_c(t)) = Q_{sw}^{i}(1.5\_sameML)\frac{1.7 - v_c}{0.2} + Q_{sw}^{i}(1.7\_orig)\frac{v_c - 1.5}{0.2} \tag{16}$$

Figure 7 shows the spray flow rates calculated by the above equation during the speed drop. Figure 8 indicates that after the speed drop, the metallurgical length gradually decreases, then increases, and finally reaches steady state after a small overshoot. The metallurgical lengths before and after the speed drop under steady state are almost the same; the deviation of the metallurgical length for spray table control under the spray patterns of '1.7_*orig*' and '1.5_*sameML*' is an undershoot of 0.92 *m* followed by an overshoot of 0.18 *m*. The metallurgical length deviation is reduced by 66.1% compared with the constant spray cooling case. The overshoot would be a potential concern for whale formation, if the metallurgical length was near the end of containment. However, this overshoot is small, within the deviation remaining at steady-state for this set of conditions.

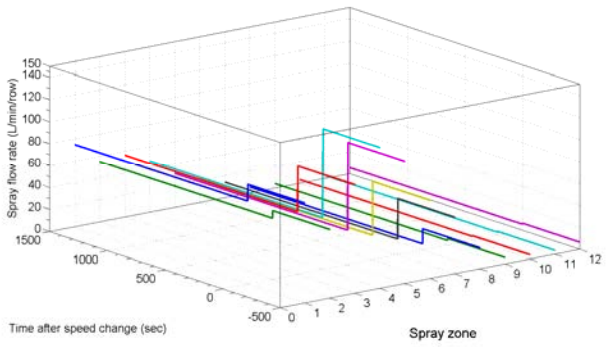

Figure 7. Flow rates under spray table control

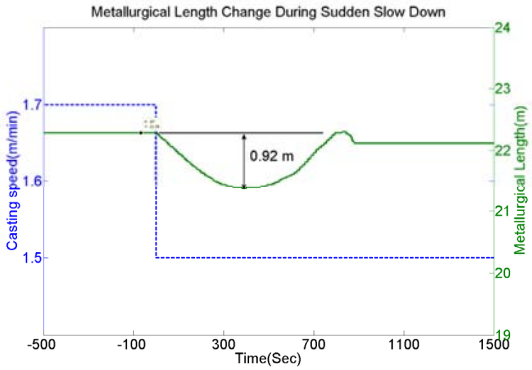

Figure 8. Model prediction of ML under spray table control

Time-constant control

The average casting speed for each zone can be calculated by equation (3); $\overline{v}_i(t)$ from the above equation is then used to calculate the spray flow rates based on the spray patterns – '1.7_*orig*' and '1.5_*sameML*':

$$Q_{sw}^{i}(t) = Q_{sw}^{i}\left(\overline{v}_i(t)\right) = Q_{sw}^{i}(1.5\_sameML)\frac{1.7-\overline{v}_i(t)}{0.2} + Q_{sw}^{i}(1.7\_orig)\frac{\overline{v}_i(t)-1.5}{0.2} \tag{17}$$

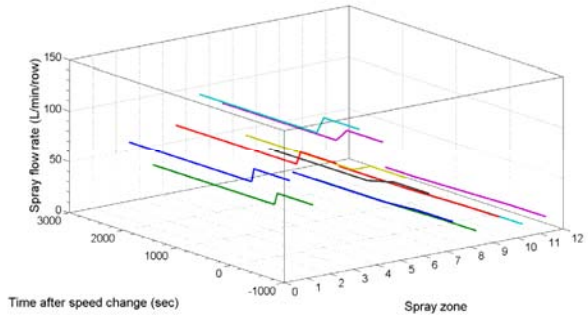

Figure 9. Flow rates under spray table control

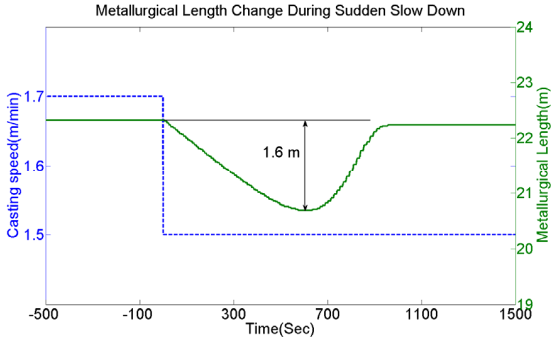

Figure 10. Model prediction of ML under spray table control

Figure 9 shows the spray flow rates calculated by the above equation during the speed drop. Figure 10 shows the metallurgical length profile under the time-constant control method; the deviation of the metallurgical length is an undershoot of 1.6 *m* with no overshoot. Compared with the constant spray cooling case, the metallurgical length deviation is reduced by 41.2%. Compared with Figure 8, the metallurgical length deviation of time-constant control is larger than the result under spray table control. This is because the flow rates calculated by the time-constant method change gradually; thus during the transition, the steel receives more water; thus, more heat is extracted by spray cooling water, and this leads to smaller minimum metallurgical length and larger metallurgical length deviation.

Bang-bang control

Single-step bang-bang control

For single-step bang-bang control, the water flow rates in the spray zones switch only once. To implement this as a real control method, the metallurgical lengths before and after speed change should be the same, then the water flow rate of spary zone *i* is calculated by:

$$Q_{sw}^{i} = \begin{cases} Q_{sw}^{i}(1.7\_orig)\ if\ \ t < t_{1b}^{i} \\ Q_{sw}^{i}(1.5\_sameML)\ if\ \ t \geq t_{1b}^{i} \end{cases} \tag{18}$$

To achieve minimum metallurgical fluctuation, the flow rates at each zone need to drop immediately after speed drop, i.e. $t_{1b}^{i} = 0$, then this method is identical to spray table control.

For all two-step and three-step bang-bang control sequences, the first switch is the same, i.e. after the speed drop, the flow rates immediately drop to the minimum flow rates allowed for all spray zones to minimize the heat removal and shell growth. It is vital to study the effect of the first switch, because it affects the selection of the parameters for two-step and three-step bang-bang control sequences.

In this section, the first switch of the other two bang-bang control sequences is studied. The flow rates for different spray zones under single-step bang-bang control are described in equation (4), with $t_{1b}^{i} = 0$ for all spray zone *i*. Figure 11 shows the CONONLINE model prediction of the average shell thickness in zone 1-9 for single-step bang-bang control, zone 10-12 is neglected because the steel strand is already fully solid before entering zone 10.

Figure 12 shows the metallurgical length profile under single-step bang-bang control, the metallurgical length has the opposite transient behavior as the behavior of the average shell thickness shown in Figure 11. Figure 12 indicates two important findings: (1) the minimum undershoot of the metallurgical length possible is 0.8 *m*, (2) in order to keep metallurgical lengths under steady state the same, two-step bang-bang control with second switch to be the flow rates in spray pattern '1.5_*sameML*' should be applied.

Two-step bang-bang control

Two-step bang-bang control is introduced and in order to match the metallurgical lengths at steady state for the two casting speeds, the second step (final) flow rates are chosen to be the flow rates from the spray pattern '1.5_*sameML*', which achieves the same metallurgical length as '1.7_*orig*'. Therefore, from equation (5), the parameters that need to be chosen are switching times t_{2b}^{i} for all spray zones. The switching times can vary for different spray zones.

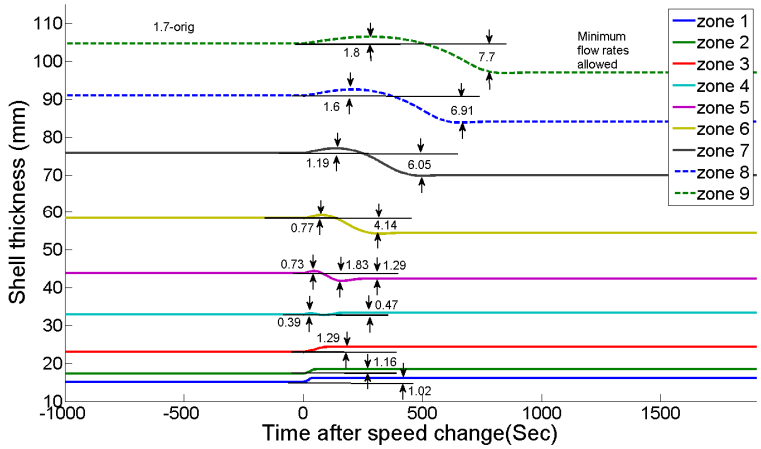

Figure 11. Model prediction of average shell thickness of all spray zones under single-step bang-bang control

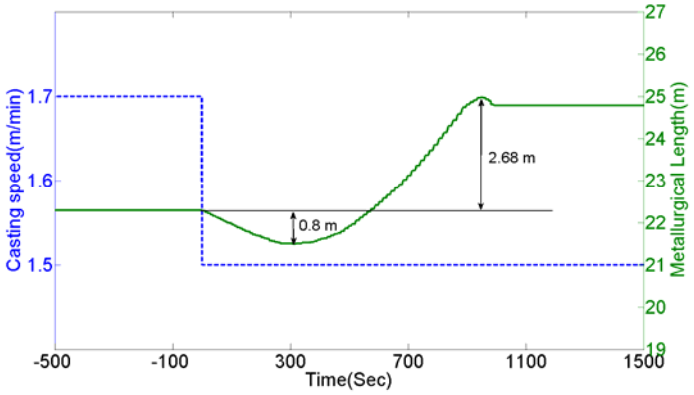

Figure 12. Model prediction of metallurgical length under single-step bang-bang control.

The relation between the shell thickness and the metallurgical length is clear: the metallurgical length is determined by the shell thickness profile of the spray zone in which the steel strand becomes fully solid, i.e. zone 9 in this case. However, the shell thickness behavior in the upper zones will affect the behavior in zone 9. Therefore, the switching times of the second switch t_{2b}^{i} were tuned sequentially and separately for every spray zone based on the average shell thickness profile of the corresponding zone. Equation (5) then becomes the following:

$$\begin{aligned}
&\textit{for i=1-3: } Q_{sw}^{i}(t)=\begin{cases} Q_{sw}^{i}(1.7_orig) & \textit{if } t<t_{2b1}^{i} \\ Q_{sw}^{i}(1.5_sameML) & \textit{if } t\geq t_{2b1}^{i} \end{cases} \\
&\textit{for i=4-9: } Q_{sw}^{i}(t)=\begin{cases} Q_{sw}^{i}(1.7_orig) & \textit{if } t<t_{2b1}^{i} \\ Q_{sw}^{i}(min) & \textit{if } 0\leq t\leq t_{2b2}^{i} \\ Q_{sw}^{i}(1.5_sameML) & \textit{if } t\geq t_{2b2}^{i} \end{cases} \\
&\textit{for i=10-12: } Q_{sw}^{i}(t)=\begin{cases} Q_{sw}^{i}(1.7_orig) & \textit{if } t<0 \\ Q_{sw}^{i}(1.5_sameML) & \textit{if } t\geq 0 \end{cases}
\end{aligned} \tag{19}$$

where the switching times for zone 1-9 are shown in Table 5.

Table 5. Switching time of the modified two-step bang-bang control sequence

Zone (i)	$t_{2b1}^{i}(\text{sec})$	$t_{2b2}^{i}(\text{sec})$
1	0	\
2	0	\
3	0	\
4	0	30
5	0	48
6	0	80
7	0	140
8	0	180
9	0	296

The flow rates under the two-step bang-bang control sequence are shown in Figure 13. The model prediction of the metallurgical length history is shown in Figure 14, with maximum metallurgical length deviation of 0.8 *m*. Compared with the constant spray cooling case, the metallurgical length deviation is reduced by 70.6%. However, there is a small overshoot (0.37 *m*) before reaching steady state, which is unable to be removed with two-step bang-bang control sequence while still maintaining the 0.8 *m* maximum metallurgical length deviation. The reason is that, to remove the overshoot, for the slice which have the maximum metallurgical length - slice (2.54) (which is 2.54 m away from the meniscus when the speed drop happens), to receive more cooling water. Figure 15 shows the flow rate history of slice (2.54); the results show that the flow rates in zone 5-9 have already reached the values from the spray pattern of '1.5_*sameML*' when slice (2.54) enters the spray

zones. If more cooling water is needed for slice (2.54), the flow rate in zone 4 need to be increased, i.e. decrease t_{2b2}^4, but this might increase the metallurgical length deviation per the previous discussion.

To better straighten out the response (decrease the overshoot), three-step bang-bang control is considered: full step down, a bit earlier strong step up and then small step down. In the other parts of this work, the two-step bang-bang control method refers to the modified two-step bang-bang control method.

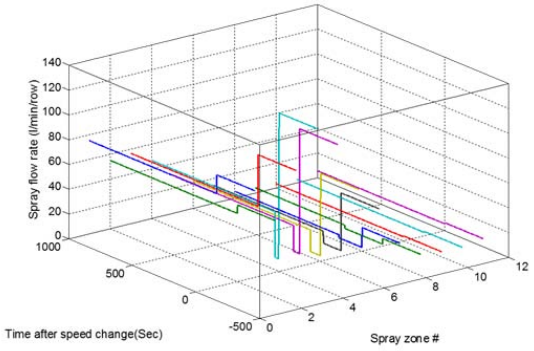

Figure 13. Flow rates of two-step bang-bang control

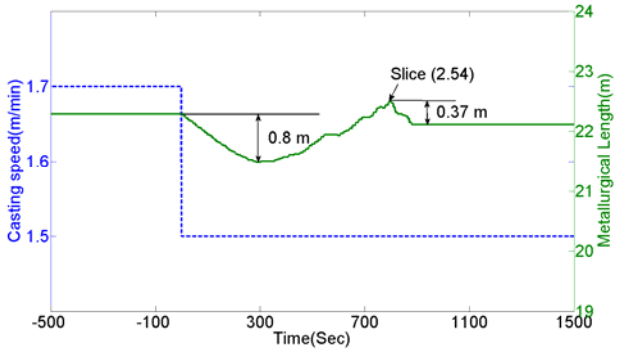

Figure 14. Model prediction of ML under two-step bang-bang control

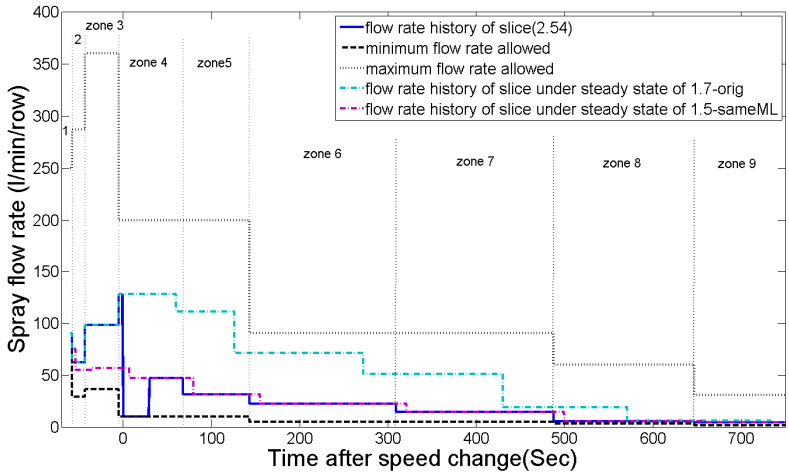

Figure 15. Flow rate history for slice (2.54) shown in Figure 14.

Three-step bang-bang control

To reduce the overshoot shown in the metallurgical length profile in Figure 14, another bang-bang control sequence, which added a third sudden step (switch) to the two-step bang-bang control sequence, is applied to the model. In three-step bang-bang control, there are three sets of parameters to be determined: $t_{3b2}^i, t_{3b3}^i, Q_{sw}^i(3b)$. The first switch is assumed to occur at the time of speed drop, t_{1b}, in all cases.

From the discussion in the previous section, to reduce the overshoot, the amount of spray cooling water received by slice (2.54) in spray zone 4 needs to be increased. Therefore, three-step bang-bang control is first only applied in zone 4, and two-step bang-bang control sequence is applied in the rest zones. $Q_{sw}^4(3b)$ is chosen to be 98.2 *L/min/row*, t_{3b}^4, t_{3b2}^4 are chosen to be 30 *secs* and 60 *secs*, this set of parameters give roughly the same amount of cooling water for slice (2.54) in zone 4 as in '1.5_*sameML*'. The metallurgical length transient behavior of the above case is shown in Figure 16. The result shows that the slice that has maximum metallurgical length is now slice (3.74). The metallurgical length for slice (2.54) and the slices near it were reduced. Although the spray flow rate in the spray zone 4 was tuned specially for slice (2.54), the spray flow rate in the whole zone is changed and affected the other slices in zone 4. Now repeat the same method for slice (3.74), by this tuning method, the set of parameters listed in Table 6 are finally chosen.

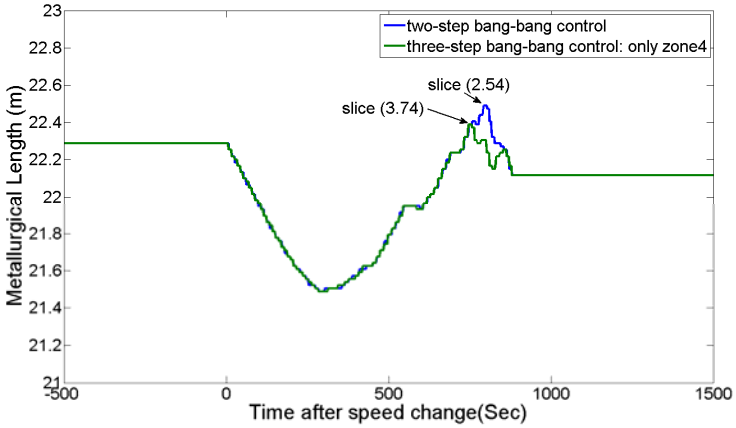

Figure 16. Comparison of ML for two-step bang-bang control sequence and three-step bang-bang control sequence only applied in zone 4

Table 6. Parameters of three-step bang-bang controller

Zone (i)	$t^i_{3b1}(\text{sec})$	$t^i_{3b2}(\text{sec})$	$t^i_{3b3}(\text{sec})$	$Q^i_{sw}(3b)$ ($L/min/row$)
1	0	\	\	\
2	0	\	\	\
3	0	\	\	\
4	0	30	60	98.2
5	0	48	110	55
6	0	80	130	30
7	0	110	140	20

The equation (6) is then modified to the following:

$$\text{for i=1-3: } Q^i_{sw}(t)=\begin{cases} Q^i_{sw}(1.7\_orig) & if\ t<t^i_{3b1} \\ Q^i_{sw}(1.5\_sameML) & if\ t\geq t^i_{3b1} \end{cases}$$

$$\text{for i=4-7: } Q^i_{sw}(t)=\begin{cases} Q^i_{sw}(1.7\_orig) & if\ t<t^i_{3b1} \\ Q^i_{sw}(min) & if\ 0\leq t\leq t^i_{3b2} \\ Q^i_{sw}(3b) & if\ t^i_{3b2}\leq t\leq t^i_{3b3} \\ Q^i_{sw}(1.5\_sameML) & if\ t\geq t^i_{3b3} \end{cases} \quad (20)$$

$$\text{for i=8-9: } Q^i_{sw}(t)=\begin{cases} Q^i_{sw}(1.7\_orig) & if\ t<t^i_{2b1} \\ Q^i_{sw}(min) & if\ 0\leq t\leq t^i_{2b2} \\ Q^i_{sw}(1.5\_sameML) & if\ t\geq t^i_{2b2} \end{cases}$$

$$\text{for i=10-12: } Q^i_{sw}(t)=\begin{cases} Q^i_{sw}(1.7\_orig) & if\ t<0 \\ Q^i_{sw}(1.5\_sameML) & if\ t\geq 0 \end{cases}$$

The flow rates history of all spray zones are shown in Figure 17. The result of the metallurgical length profile under three-step bang-bang control sequence is shown in Figure 18. Same as two-step bang-bang control sequence, the maximum deviation of metallurgical length is 0.8 *m*. Compare with the constant spray cooling case, the metallurgical length deviation is reduced by 70.6%. There is still a small overshoot (0.1 *m*) in the metallurgical length profile, but the slice (0.8), which has maximum metallurgical length in the overshoot region, is still in the mold when the speed change happens. When it enters each spray zones, the spray flow rates are already in steady state of '1.5_*sameML*', which means the overshoot is not caused by the secondary cooling but the primary cooling.

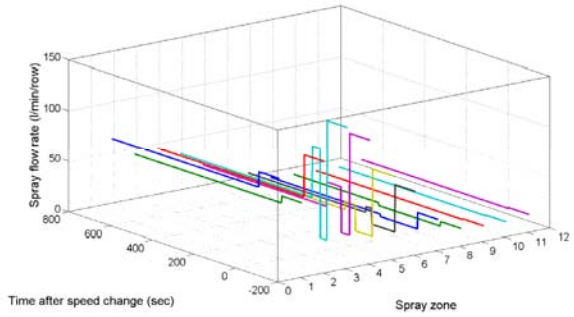

Figure 17. Flow rates of three-step bang-bang control

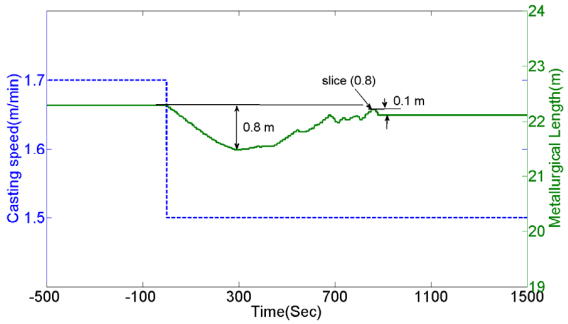

Figure 18. Model prediction of ML under three-step bang-bang control

DISCUSSION

For the objective of controlling metallurgical length control, it is only feasible to achieve constant metallurgical length for a small speed drop of 0.2 *mm/min* from 1.7 to 1.5 *m/min*, for a typical thick slab caster. Spray table control based on spray patterns of '1.7_*orig*' and '1.5_*sameML*' are close to the maximum and minimum flow rates, and thus produce a significant increase in surface temperature for the lower speed. This reduces the maximum deviation of the metallurgical length by 66.1%, decreasing the undershoot from 2.72 *m* (with no control) to 0.9 *m*.

The time-constant control method based on the same spray patterns reduces the maximum deviation of metallurgical length by only 41.2%. Thus, time-constant control is not as good at controlling metallurgical length, although it is much better than spray-table control at maintaining surface temperature during the speed change.

Two-step and three-step bang-bang control sequences produce maximum metallurgical length dips of 0.8 *m*, reducing the metallurgical length undershoot by 70.6%. Thus, the bang-bang control sequences have better performance at maintaining the metallurgical length. Moreover, three-step bang-bang control has no overshoot of the metallurgical length profile. Overall, the three-step bang-bang control sequence has the best performance at controlling the metallurgical length during the speed drop among all the methods studied. However, this method causes sudden changes in the surface temperature profile which are very likely to cause cracks. So, this method is likely not the most optimal control method overall. Further work is needed to evaluate the different control methodologies for different control objectives together.

CONCLUSIONS

In this paper, the behavior of the metallurgical length during a sudden drop in casting speed was investigated with four different types of control methods. Simulation results demonstrate that the controllability of the metallurgical length is limited even for a small speed drop of 0.2m/min. Bang-bang control has the best performance with minimum metallurgical length deviation of 0.8 *m*. Sudden speed change is not recommended. Further work is needed to evaluate control methodologies for different control objectives together.

REFERENCES

[1] J. Brimacombe, P. Agarwal, S. Hibbins, B. Prabhaker and L. Baptista, "Spray Cooling in the Continuous Casting of Steel," *ISS/AIME*, pp. 109-123, 1984.

[2] Z. Dou, Q. Liu, B. Wang, X. Zhang, J. Zhang and Z. Hu, "Evolution of control models for secondary cooling in continuous casting process of steel," *Steel Research International*, vol. 82, no. 10, pp. 1220--1227, 2011.

[3] L. Klimes and J. Stetina, "Challenges in numerical modelling of continuous steel casting - very fast GPU dynamic solidification model and its use in continuous casting control," in *European Continuous Casting Conference*, 2014.

[4] J. Sirgo, R. Campo, A. Lopez, A. Diaz and L. Sancho, "Measurement of Centerline Segregation in Steel Slabs," in *IEEE Industry Applications Conference*, 2006.

[5] B. Petrus, K. Zheng, X. Zhou, B. G. Thomas and J. Bentsman, "Real-Time Model-Based Spray-Cooling Control System

for Steel Continuous Casting," *Metallurgical and Materials Transactions B*, vol. 42, no. 1, pp. 87-103, 2011.

[6] D. Liberzon, Calculus of Variations and Optimal Control Theory: A Concise Introduction, Princeton University Press, 2011.

[7] B. Petrus, D. Hammon, M. Miller, B. Williams, A. Zewe, Z. Chen, J. Bentsman and B. G. Thomas, "New Method to Measure Metallurgical Length and Application to Improve Computational Models," *Iron and Steel Technology*, vol. 12, no. 12, pp. 58-66, 2015.

[8] N. Gregurich, G. Flick, R. Moravec and K. Blazek, "In-depth Analysis of Continuous Caster Machine Behavior During Casting with Different Roll Gap Taper Profiles," *Iron and Steel Technology*, vol. 9, no. 12, p. 62, 2012.

[9] P. Duvvuri, B. Petrus and B. G. Thomas, "Correlation for Mold Heat Flux Measured in a Thin Slab Casting Mold," in *Proceedings of AISTech 2014*, Indianapolis, IN, 2014.

[10] T. Nozaki, J. Matsuno, K. Murata, H. Ooi and M. Kodama, "A Secondary Cooling Pattern for Preventing Surface Cracks of Continuous Casting Slab," *Transactions of the Iron and Steel Institute of Japan*, vol. 18, no. 6, pp. 330-338, 1978.

ACKNOWLEDGEMENT

This work was supported by NSF Grant # 1300907 and the Continuous Casting Consortium at the University of Illinois at Urbana-Champaign. Special thanks are given to JFE Steel Corporation for providing caster data and casting conditions.